INTERNATIONAL JOURNAL OF SUSTAINABLE CONSTRUCTION ENGINEERING AND TECHNOLOGY
ISSN: 2180-3242 e-ISSN: 2600-7959

IJSCET

Vol. 15 No. 2 (2024) 123-135
https://publisher.uthm.edu.my/ojs/index.php/ijscet

Structural Behaviour of Reinforced Concrete Beams Made of Selected Waste Glass and Ceramic Tiles

Abubaker M Alamleeh[1, 2*], Stanley M Shitote[2], Timothy Nyonboi[2]

[1] *Department of Civil Engineering, Faculty of Engineering, Omdurman Islamic University, Khartoum, P.O.Box 382, SUDAN*

[2] *Institute for Basic Sciences, Technology and Innovation, Pan African University, Nairobi, P. O. Box 62000 00200, KENYA*

*Corresponding Author: abubaker.almaleeh@oiu.edu.sd
DOI: https://doi.org/10.30880/ijscet.2024.15.02.011

Article Info

Received: 14 June 2023
Accepted: 01 February 2024
Available online: 11 March 2024

Keywords

Glass, ceramic tiles, reinforced, concrete, ANSYS, non-conventional concrete

Abstract

Worldwide, construction and demolition wastes contribute the most wastes. Hence, environmental concerns have been raised, and more investigations have been recommended for recycling potential. Glass and Ceramic wastes are currently disposed of in landfills. This paper aims to study the structural behaviour of non-conventional concrete made of waste glass and ceramic tiles. A comparison is conducted between the normal and non-conventional concrete beams. The non-conventional concrete is made by replacing normal sand and gravel at 25% and 50% percentages. Both glass and ceramic tiles are used separately and blended in three different types (A, B, & C) of concretes. The laboratory experiments are verified with a Finite Element model for the three reinforced concrete types using ANSYS software. The results of conducted comparison shown that the non-conventional reinforced concretes have acceptable consistent with the normal reinforced concrete, and the reuse of glass and ceramic waste is technically feasible.

1. Introduction

Presently, world countries produce annually about 1.3 billion tonnes of solid waste. This volume is expected to rise up to approximately 2.2 billion tonnes by 2025 (Dahlén, Management, & 2010). Globally, the production of ceramic tiles during 2011-12 was about 11,166 million square meters (Zimbili, Salim, & Ndambuki, 2014). In 1994, about 9.2 million metric tons of waste glass is discharged in the United States (Chesner, Collins, & MacKay, 1997). Therefore, recycling of waste glass and ceramic tiles wastes has generated considerable recent research interest as potential alternative aggregates to gravel and sand.

Ceramic tiles and glass originally are manufactured from clay and sand, respectively, and normally are used in many different ways in life (ASTM C373-88, 2006). Waste ceramic tiles and glass are suitable materials to be recycled, especially in concrete (Almaleeh A. M., 2019). The research outcomes of using the waste ceramic tiles and glass as aggregates encourage researchers to emphasize the potential of utilizing them in structures. However, the structural behaviour of the reinforced concrete which made of waste ceramic tile and glass as aggregate needs more investigation. And there has been no detailed investigation of load-deflection behaviour of such a concrete.

There are relatively few previous studies in the use of waste ceramic tiles and glass in concrete as aggregate. These studies showed that the physical and mechanical properties are appropriate under some conditions for applications in the construction industrial. The waste glass was tested as aggregate (Meyer and Baxter, 1998;

Wright, J. R et al., 2014; Shi, C., & Zheng, K. (2007).; Ling, T. C., Poon, C. S., & Wong, H. W., 2013; Topcu and Canbaz, 2004; Chen et al., 2006; Almaleeh et al, 2019).

Recently, some researchers investigate the replacement of sand with lower percentages and they studied the load-displacement, and failure behaviour. Jad Bawab et al., (2021) replaced glass waste f cathode-ray tubes (CRTs) partially for sand. Four concrete mixes were made with 0%, 10%, 20%, and 30% CRT glass waste as a partial replacement for sand. Compressive and flexural strengths, and modulus of elasticity were all increased in concrete containing CRT glass, notably at a 10% replacement level. Additionally, when 10% of the sand is replaced, the load carrying capability is increased when compared to the control beam and beams with 20% and 30% CRT glass replacement. The beams' failure mode and tensile damage are similar to the results of the experimental investigation. Sheelan Mahmoud Hama et al., (2019) investigated the effect of using glass powder as a replacement for cement in the following weight percentages: 0 percent (reference), 10%, and 15%. When compared to reference beams, glass powder-filled beams demonstrated good resistance and flexural performance.

Atoyebi, O. D. et al., (2018), These researches concluded that the glass can be used suitably in concrete as aggregate with no much change appeared on the mechanical properties of concrete.

On the other hand, (Hooton & Khaloo, 1999; Senthamarai & Devadas Manoharan, 2005; Zimbili et al., 2014; Binici, 2007; Correia, De Brito, & Pereira, 2006; García-González, Rodríguez-Robles, Juan-Valdés, Morán-Del Pozo, & Guerra-Romero, 2015; Almaleeh et al, 2019) have indicated that the waste ceramic tiles have a high potential to be used in structural concrete. The performance of the concrete contains waste ceramic tiles is even better than conventional concrete, especially in properties such as; density, durability, permeability, compressive strength, and tensile strength. However, there remains a need to study, the blind of waste ceramic tiles and glass at the same time has not been covered in the literature review. In addition, properties such as; bending, crack patters, and deflection parameters have not been evaluated.

Much of the greater part of the literature on lacks clarity regarding the structural behaviour of nonconventional concrete. Therefore, this paper presents in detail; the structural behaviour of non-conventional reinforced concrete which are made from glass and ceramic tiles. The non-conventional concrete is tested experimentally in the laboratory. It also provides a Finite Element Model (FEM) of the beam elements which conducted through the ANSYS program (Ansys, 2012). Numerical model is applied to simulate the behaviour of four full-size beams from linear through nonlinear response and up to failure. The comparison between the FEM and the laboratory experiment is demonstrated and discussed. This comparison is illustrated in terms of load-deflection behaviour for different types of concretes. The critical locations on the beams are selected to be measured such as; load-deflection plots at mid-span; first cracking loads; loads at failure; and crack patterns at failure. The models are subsequently expanded to encompass the nonlinear behaviour of the suggested beams. Modelling simplifications and assumptions developed during this research are presented. Conclusions from the current research efforts and recommendations for future studies are included.

2. Materials and Method

2.1 Materials

Concrete class 25 with Portland cement CEM 32.5 is targeted. River sand and crushed stone are used as normal aggregates. In addition to that, waste ceramic tiles and glass are crushed manually as in Fig. 1, and then used as aggregates to replace the conventional sand and gravel. Fine and coarse aggregates are replaced by crushed ceramic tiles and glass to made three types of non-conventional concretes as in Table 1. The gradation of crushed ceramic tiles and glass is suitable and fall between the limits as shown in Fig.2. In our previous research, (Almaleeh A. M. at el., 2019) these three types of concretes gave suitable results in compressive, tensile splitting, and flexural strengths. The replacement of normal sand and gravel is demonstrated in Table 1. Sand and gravel are replaced by mixed waste glass and ceramic tiles in Type A and B, meanwhile, in Type C only ceramic tiles are replaced.

Int. J. of Sustainable Construction Engineering and Tech. Vol. 15 No. 2 (2024) p. 123-135

Fig. 1 *Fine and coarse waste glass and ceramic tiles*

2.2 Mix Design

Two mix design methods are applied and compared, the Department of Environment (DoE) method and American Concrete Institute method (ACI 211.1) (ACI 211.1-91, 1997). The DoE design method was introduced in 1950, under the name "Road Note No 4", which later renamed "Design of Normal Concrete Mixes" by the British Department of Environment (DoE) in 1975. This design guidance, which is often referred to as the British Standard concrete mix design, was revised in 1988 to reflect changes to the then current British Standards (BS 5328—Concrete, Part 2.)

Table 1 shows the approximate composition of concrete, and replacement of the aggregates. ACI 211.1-91 recommended that trial batches in the laboratory should be conducted, to check the first assumed proportions. In our previous research, these values gave the optimum replacement for normal aggregates.

Table 1 *Percentages of the components for different suggested types of concrete*

Concrete type	Sand (%)	Gravel (%)	Fine ceramic (%)	Fine glass (%)	Coarse ceramic (%)	Coarse glass (%)
A	50	100	25	25	0	0
B	50	75	25	25	25	0
C	50	75	50	0	25	0

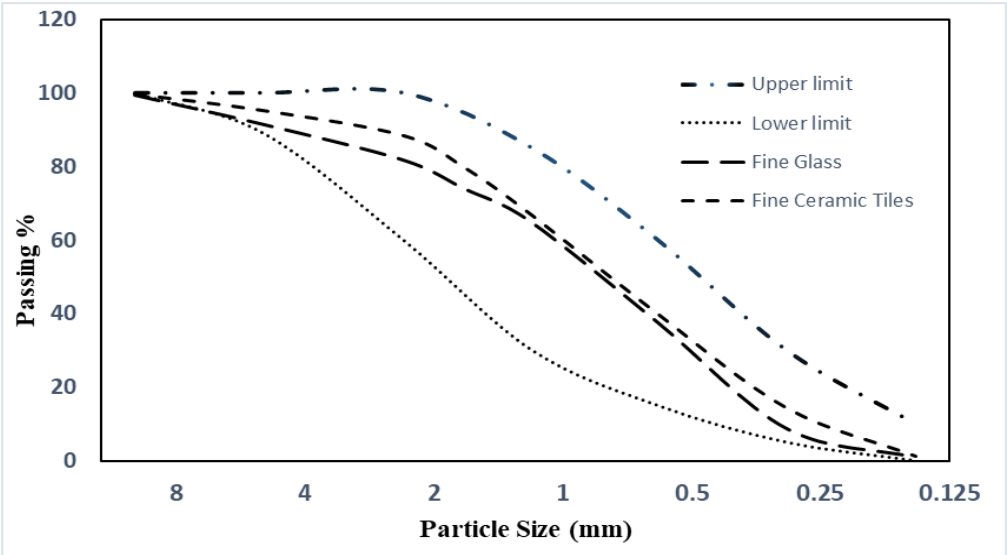

Fig. 2 *Particles gradating curve of fine glass and ceramic tiles*

2.3 Materials Properties

Concrete

Applying a FEM using ANSYS obtained more data on the behaviour of the concrete. Concrete is a brittle material, and it does not get that much of elasticity as in the steel. The tensile strength of concrete ranged between 8 – 15% of the compressive strength which is not advantageous (McCormac & Brown, 2013). The concrete model needs a full stress-strain curve. Thus, it covers the nonlinear behaviour of the concrete. The linear line in the graph using the concrete modulus of elasticity (Ec), and the unit weight of concrete (Wc) is varying from 1500 – 2500kg/m3.

$$E_c = w_c^{1.5}(0.043)\sqrt{f_c^`} \quad (1)$$

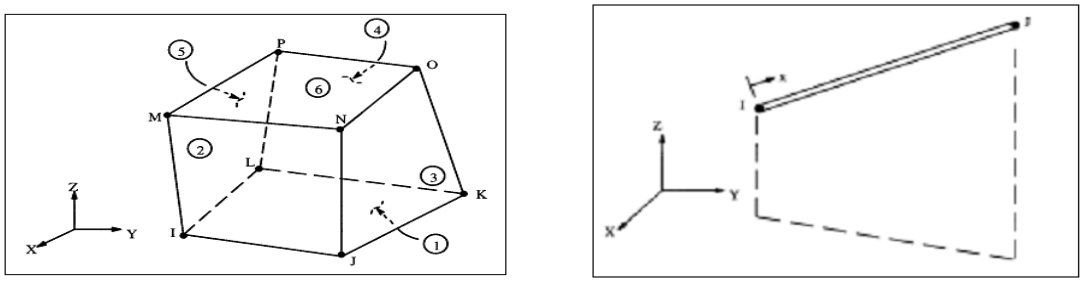

(a) **(b)**

Fig. 3 *(a) Solid65 – 3D Reinforced concrete, (b) Steel Reinforcement element, Link8 with two nodes, 3D*

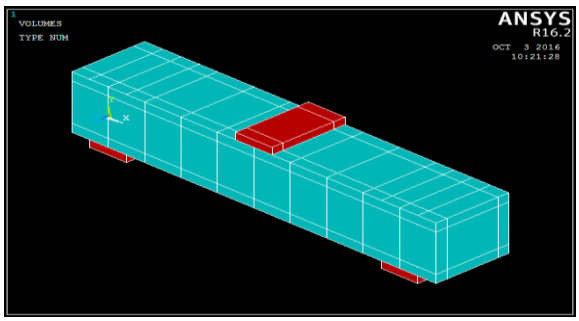

Fig. 4 *3D beam model*

For nonlinear static analysis, the load is applied gradually. The first part of the curve, and up to about 30% of the ultimate strength $f_c^`$, it can be considered essentially linear. After it reaches the maximum strength, the curve descends into a softening region the peak compressive stress point. In tension, the concrete is linear up to maximum tensile strength.

Modulus of elasticity of the concrete was obtained experimentally for the four different types of concrete. Because it served as input in the ANSYS program. The nonlinear region is modelled as multi-linear. The uniaxial compressive stress – strain relationship for concrete is used which has been obtained by the numerical expression (Desayi, P. and Krishnan, 1964). Equations 2 and 3 are used. Also, Hooke's law equation 4 was used to represent the stress – strain curve.

$$f = \frac{E_c \varepsilon}{1+\left(\frac{\varepsilon}{\varepsilon_o}\right)^2} \quad (2)$$

$$\varepsilon_o = \frac{2f_c^`}{E_c} \quad (3)$$

Int. J. of Sustainable Construction Engineering and Tech. Vol. 15 No. 2 (2024) p. 123-135

$$\varepsilon_o = \frac{f}{E_c} \quad (4)$$

Where:

f = stress at any strain ε.

ε = strain at stress f.

ε_o = strain at the ultimate strength $f_c^{`}$.

In addition, ANSYS required other input data for modelling the concrete such as; ultimate uniaxial tensile strength (modulus of rupture, fr), Poisson's ratio (ν), and shear transfer coefficient (βt). modulus of rupture can be obtained from equation 5 (Ohbuchi & Obikawa, 2001).

$$f_r = 0.7\sqrt{f_c^{`}}\ (\text{MPa}) \quad (5)$$

Poisson's ratio of concrete varied from 0.18 - 0.2. Shear transfer coefficient denotes forms of the crack face. Its value ranged between 0.0 – 1.0. Zero value means smooth cracks, and 1.0 indicating rough cracks (Ansys, 2012). The βt value that was used in several studies of modelling reinforced concrete is between 0.05 and 0.25 (Ohbuchi & Obikawa, 2001)

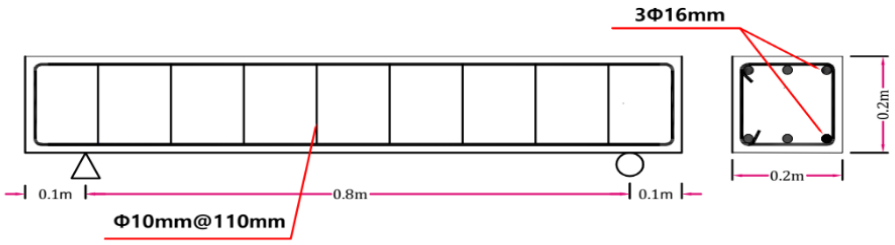

Fig. 5 *Tested Loading and boundary conditions on the beam*

2.4 Steel Reinforcement and the Support Plate

The steel reinforcement Grade 60 is used, with modulus elasticity of 200,000MPa, and 0.3 Poisson's ratio. For the finite element model, steel reinforcement assumed to be modelled as an elastic-perfectly plastic material (Bilinear). Thus, the yield stress of the steel f_y is 460 MPa. The amount of steel rebar is 3T16 (top and bottom) for longitudinal reinforcement, and the T10 stirrups with spacing 110 mm as shown in Fig. 5. All beams have a square cross-section of 200mm×200mm and length of 1000 mm.

Steel plates are used as supports, and it is modelled as linear elastic materials with an elastic modulus of 200,000 MPa, and Poisson's ratio of 0.3. Therefore, it could be given more stress distribution on the contact area between the concrete and the plate. Table 2, summarized the properties of the material that are used in ANSYS.

3. Test Set- Up and Instrumentation

3.1 Experimental Test

The investigation of the flexure behaviour of four samples reinforced non-conventional concrete beams is done according to BS 1881-118:1983. Four samples are cast for each type of concrete. A total of 16 beams samples are cast for the four different types of concrete in the experiment.

Three point-loads are subjected to the beams. In addition, strain gauges are attached on the beams at specific locations; at the bottom and at the top fibre of the beam; on both sides of the beams in the high shear region, to record the strain. LVTD is fixed in the middle of the beam to record the maximum vertical displacement. Load cells are used in order to apply the load gradually. Fig. 6 shows the experimental set up for a beam. Lastly, the compression and tensile splitting strengths of concrete for all different types are conducted according to BS 1881-116:1983, BS 1881-117:1983 respectively, Fig. 5 shows the details of the tested beams.

The beams are tested under a three-point loading system. The net span of beam was 800 mm, and 100mm space between the support and the beam outer face. A 150 kN load is applied by a hydraulic jack. Dial gauges are used to measure the vertical displacement: two dial gauges with one point load are positioned with an accuracy

of 0.01 mm, and one gauge with a resolution scale of 0.001mm is set up at the middle of specimens. A testing machine is used to set the loading rate, and recorded values are then obtained.

Strain gauges located 200 mm from the edge of the beam are used to calculate the elongation in the concrete. In addition, three sensors are installed at 0°, 45°, and 90° as rosette sampler, and a fourth one is positioned at the middle of beam to evaluate the bending strain. The cable splices with strain gauges are then soldered together, and the sensors are tied to the specimen surface using adhesive materials. Electric wires with a length of 3m are used as another channel side connection for data logger. The load and sensor readings are then recorded using a camera that is focused on the dial gauges and a data logger, respectively, as shown in Fig. 4.

Fig. 6 *Simply supported beam subjected to three points load*

4. Finite Element model

Nonlinear static analysis is conducted using ANSYS finite element program. ANSYS is utilized in this study to simulate the behaviour of experimental beams. Concrete is modelled as solid65 as in Fig. 3. The steel reinforcement is modelled as link8, and in ANSYS each element defines two nodes at the end.

Solid65 has eight nodes with three degrees of freedom at each node translations in the nodal x, y, and z directions. It is capable of plastic deformation, cracking in three directions, and crushing. The geometry and node locations for this element type are illustrated in Fig. 4.

Solid185 is used to model the two simple supports at the bottom. The element has 8 nodes, and each node has three degrees of freedom in three dimensions x, y, and z. The geometry and the locations of the nodes are similar to solid65 (Ansys, 2012).

This step in ANSYS called meshing, it discretizes the beam into small elements depending on the required accuracy. The number of elements gave more accurate results. (Ohbuchi & Obikawa, 2001) performed a comparison between the ANSYS and the SAP2000 program. That comparison showed that when the number of elements increased, the accuracy of the results increased. This step also signs the defined materials for each element. In this model, the beam is discretized into elements as in Fig.7 with a size of 50mm.

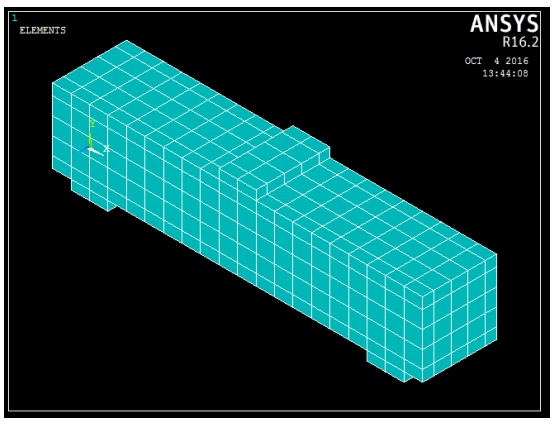

Fig. 7 *Discretized 3D beam into element*

Int. J. of Sustainable Construction Engineering and Tech. Vol. 15 No. 2 (2024) p. 123-135

4.1 Loading and Boundary Conditions

After meshing the beam and sign the defined materials, the volumes, lines, and nodes are merged. Thus, any replicate in the model which can influence the solution is removed. This step followed by applying the load and boundary conditions. Concentrated loads (20,000 N) are implemented in each node in the middle of the beam. So, the total load on the beam will be the summation of the applied load at the nodes. Supports are assumed to be hinge at one support and a roller at the other support. Hinge support singed by stopping the displacement in x, y, and z, while roller support signed by stopping the displacement in the longitudinal axis of the beam (x axis in our model).

4.2 Solve The Model

The solution of the model is formed to obtain a linear and nonlinear solution. Normally, the total load is divided into load steps. The load is increasing incrementally at each next step until the beam fails. The program allows one to select the number of iterations at each sub-step. ANSYS uses Newton Raphson equilibrium iterations for upgrading the model stiffness at each load step. Here, the assumed maximum number of equilibrium iterations per step load is 20. For time control, the time at the end of the load step is the maximum applied load (20,000 N). The number of sub-step is considered as 25 with load step ranged between 1000 and 5000 respectively.

Table 2 *Summary of the properties of the material for concrete*

Concrete type	E_c (MPa)	$f_c^{`}$ (MPa)	f_r (MPa)	ν	βt
Control	21515	25.4	3.53	0.2	0.2
Type A	20186	24.61	3.473	0.2	0.2
Type B	22178	25.28	3.52	0.2	0.2
Type C	24653	23.17	3.37	0.2	0.2

Fig. 8 *Test of the Beam under Three-Point Load*

5. Results and Discussion

5.1 Experimental Beam Results

The beams are cast to check the structural behaviour of the different types of concrete. The results represent group two in phase three. The three types of concrete are used to cast beams; this is for the purpose of testing the structural behaviour. The vertical defection, applied load, strains at shear points, and strain at the centre are measured. Also, the modulus of elasticity is tested. The LVDT is used to measure the deflection at the centre of the beam, while the load cell was used to apply the vertical load. Fig. 8 shows how the experiment was setup and failure under load.

Fig. 9 showed the load – deflection for all types of beams, control beam, and type C concrete beam are obtained more displacement, when the subjected load between 0 and 40 kN than type A and Type B.

In the load-deflection graph (Figure 9), it can be observed that the control beam and the Type C concrete beam exhibit higher levels of displacement when subjected to loads ranging from 0 to 40 kN compared to Type A and Type B beams. This indicates that the control beam and Type C concrete beam are more responsive to applied loads within this range, resulting in greater deflection.

The variation between the curves is not significant, and lines in Fig. 9 indicate the first crack that happened in beams. The ultimate load of specimens with concrete type B and C increased up to 5.5% and 15%, respectively, compared with the control specimens (0% replacement). While the ultimate load of specimens with concrete Type A decreased to 4.8%. By contrast, the deflection for beams with concrete type C is larger than that of the reference beam. The existence of fine glass with coarse ceramic tile materials is found to enhance the bending strength. Moreover, this enhancement is facilitated by provide more roughness particle surface. Type B concrete beam cracked before the others, and at a smaller amount of deflection. Meanwhile, Type A and Type B beams start cracking at almost the same load, but at different deflections. Type A concrete started cracking before concrete Type B.

The inclusion of fine glass and coarse ceramic tile materials has been discovered to improve the bending strength of the beams. This improvement is further facilitated by increasing the roughness of the particle surfaces. Among the different types of concrete beams, Type B experienced cracking at an earlier stage and at a lower deflection compared to the others. On the other hand, Type A and Type B beams exhibited cracking at approximately the same applied load, but at different deflections. Notably, Type A concrete started cracking prior to Type B concrete.

Certainly, the control beam demonstrated the ability to sustain a higher load and larger deflection compared to the other beams. This indicates that normal concrete has a greater capacity to withstand loads in the elastic region compared to the other materials used. It is worth noting that both the control beam and Type C beam experienced cracking at a higher load than the other beam types, giving concrete Type C an advantage in terms of load-carrying capacity.

5.2 Finite Element Model

In this section, the results obtained from the ANSYS program are presented, followed by a comparison with the laboratory results. Sixteen beams were cast using three types of concrete, including normal concrete as the control. These beams were then subjected to a three-point load configuration. The primary objective was to analyze and determine the load-deflection behavior of all the different types of beams and compare them to the control material. By conducting this comparison, the performance of the created materials can be evaluated and assessed in relation to the control material.

In addition to determining the load-deflection characteristics, the maximum strain and modulus of elasticity were also calculated for the beams. The simulation incorporated material properties, such as the modulus of elasticity and ultimate compressive strength, which are provided in Table 1. These material properties were used as inputs to accurately model the behavior of the beams in the simulation. By analyzing the maximum strain and modulus of elasticity, further insights into the mechanical response and stiffness of the different beam materials can be gained.

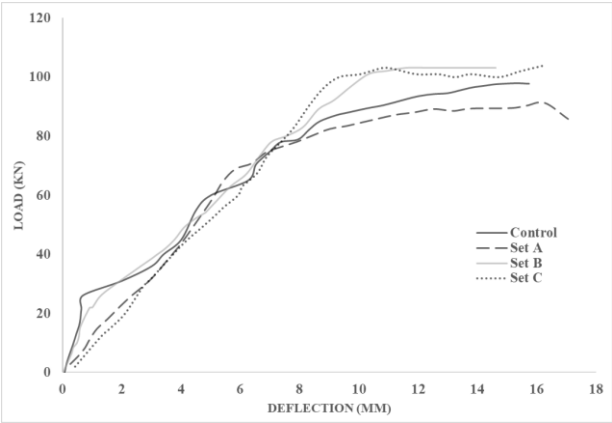

Fig. 9 *Load-Deflection of all types of beams*

5.3 Load – Deflection Curve

According to the provided information, the ultimate compressive strength of the material is 25.42 MPa, and the modulus of elasticity is 21515 N/mm^2. In Figure 10, the load-deflection behavior of the control beam is depicted, showing both the results obtained from ANSYS simulation and the experimental data. In the ANSYS simulation, the behavior closely resembled perfect elastic behavior up to approximately 30% of the ultimate compressive strength. The stress-strain curve used in the simulation was derived from experimental determination of the individual material properties. However, it's important to note that the experimental results did not exhibit the

Int. J. of Sustainable Construction Engineering and Tech. Vol. 15 No. 2 (2024) p. 123-135

same perfect elastic behavior at the beginning of the curve as predicted by the input stress-strain curve used in the ANSYS simulation.

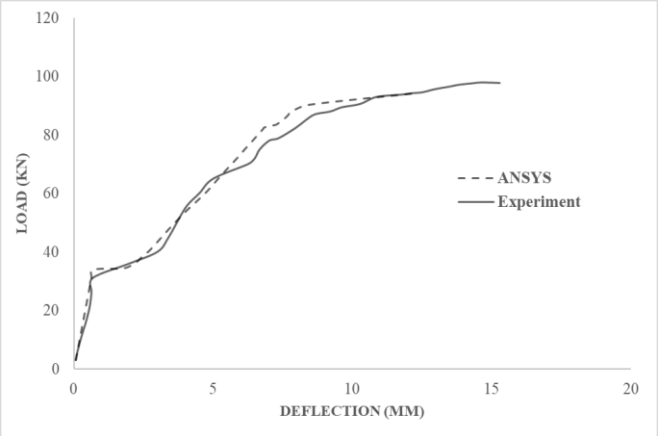

Fig. 10 *Load-deflection of the control beam*

The comparison between the simulated beam (ANSYS curve) and the experimental beam reveals that the ANSYS simulation exhibited lower deflection at lower loads, while the experimental beam started deflecting more at a lower load. This indicates a significant variation between the two curves, especially at the beginning of the load-deflection behavior. However, at a load of 94.5 kN, the two curves appear to be more conservative and show closer agreement.

In Figure 11, it is evident that concrete Type A exhibited better behavior compared to the control beam. Generally, the results obtained from the ANSYS simulation differed slightly from the laboratory results, particularly in terms of deflection at lower loads. The experimental beam demonstrated greater deflections at lower loads compared to the ANSYS simulation.

The load-deflection behavior of concrete Type B and concrete Type C are illustrated in Figure 12 and Figure 13, respectively. These figures provide insights into the specific behavior and performance of these materials compared to the control beam.

It is important to carefully analyze and interpret these variations between the simulation and experimental results to gain a comprehensive understanding of the material behavior and make informed conclusions.

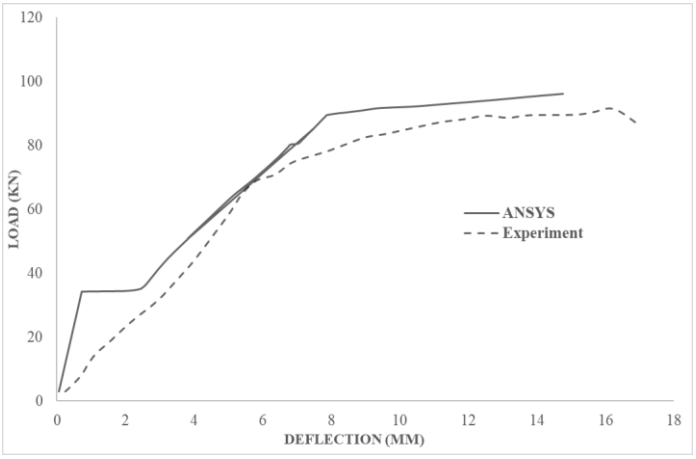

Fig. 11 *Load-deflection of Type A beam*

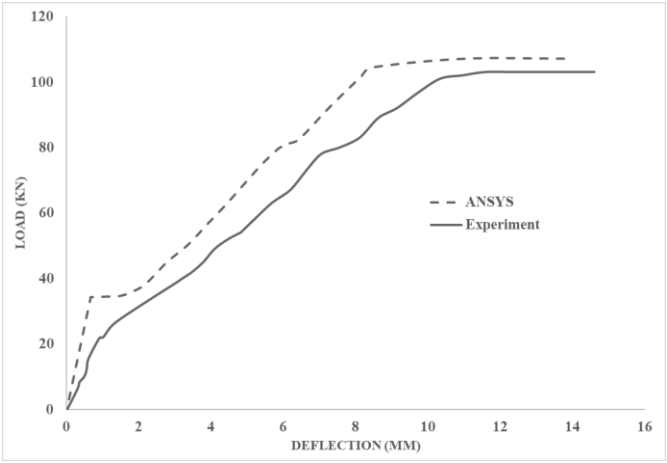

Fig. 12 *Load-deflection of Type B beam*

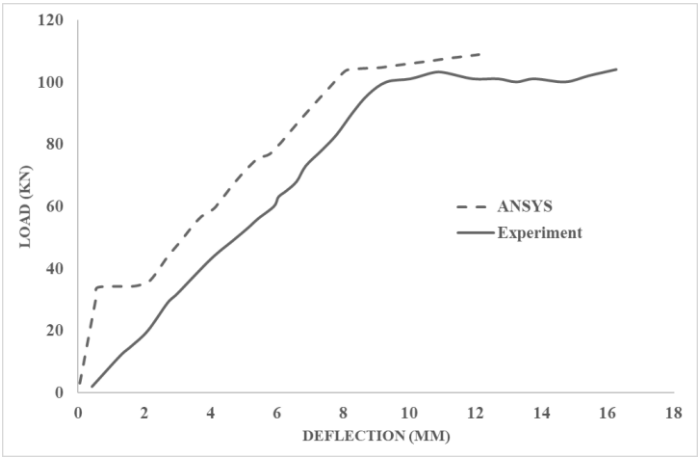

Fig. 13 *Load-deflection of Type C beam*

Indeed, the ANSYS model provided results that were comparable to the experimental data. However, it is important to consider several factors that can affect the simulation.

The concrete model used in the simulation is based on theoretical descriptions and is controlled by the modulus of elasticity. The values of modulus of elasticity are determined experimentally for each material, but they may not be highly accurate due to various factors. Additionally, the assumption that the modulus of elasticity is uniform throughout the entire section is not entirely accurate, as there can be variations in the concrete's properties. However, this assumption is often made as it is difficult to precisely control such variations.

Furthermore, the simulation assumes that the steel reinforcement is yielded throughout the reinforced section. This assumption can also influence the behavior of the beam.

Overall, while the ANSYS simulation can provide valuable insights, it is essential to consider these factors and understand their limitations in accurately representing the real-world behavior of the beams. The simulation results should be interpreted with caution, taking into account the assumptions and approximations made in the model.

5.4 The Crack Patterns of Beams

Figures 14 and 15 display the crack patterns obtained from both the ANSYS program and the laboratory experiment. It is evident that the crack patterns did not exhibit a similar pattern or direction between the two. In Fig 15, the crack patterns are depicted, and the severity of the cracks is represented by the colour changes. For example, the cracks increase in severity as the colour changes from red to green and from green to blue.

The control beam and Type C beam exhibited similar crack behaviour, with severe cracks predominantly occurring continuously at the bottom fibres of the beam. On the other hand, Type A and Type B beams showed severe cracks with a gap at the centre of the beam, which aligns with the experimental results.

These differences in crack patterns between the ANSYS simulation and the laboratory experiment indicate variations in how the two methods capture the behaviour of the beams. It's important to analyse and interpret these differences to gain a comprehensive understanding of the crack initiation and propagation in the beams.

6. Conclusion

From tests were conducted for conventional aggregates and non-conventional concrete. The following conclusions are determined;

i. The behaviour of the finite element models represented by the load-deflection charts at mid-span indicates satisfactory agreement with the experiment data, especially for Type A concrete from the full-scale beam tests. However, the finite element models show slightly more stiffness than the experiment data in both the linear and nonlinear ranges. The effects of cracks occurring in the actual beams are excluded in the finite element models, contributing to the higher stiffness of the finite element models.

ii. The ultimate loads obtained from the finite element analyses are consistently higher than the ultimate loads observed in the experimental results, with a difference ranging from 10% to 30% across the different types of concrete. Several factors contribute to this disparity. One factor is the low accuracy of the material properties data used in the analysis, which can introduce uncertainties into the simulations. Additionally, the finite element models may not fully account for the concrete's toughening mechanisms, leading to a more conservative estimation of the ultimate loads. Furthermore, certain assumptions made in modelling the material properties can introduce discrepancies between the simulated and experimental results. Overall, these factors collectively contribute to the higher ultimate loads predicted by the finite element analyses compared to the experimental results.

iii. The crack patterns observed in the finite element models at the final loads align well with the observed failure modes of the experimental beams. This indicates that the finite element analysis accurately predicts the failure behaviour of the beams. Additionally, in the case of the flexural strengthened beam, the crack pattern predicted by the finite element analysis agrees with the results obtained from hand calculations, both indicating that the beam fails primarily due to flexural stresses. This correspondence between the predicted crack patterns and the observed failure modes demonstrates the reliability of the finite element analysis in capturing the structural response and failure mechanisms of the beams.

Acknowledgement

We thank the Structural Engineering Laboratory at Jomo Kenyatta University of Agriculture and Technology where all tests described in this paper were conducted. We also thank the Management of Pan African University, Institute for Basic Sciences, Technology and Innovation. This research is funded by the African Union, Pan African University, Institute for Basic Sciences, Technology and Innovation.

References

Almaleeh, A. M., Shitote, S. M., & Nyomboi, T. (2019). The use of waste glass and ceramic tiles in concrete as aggregate. Materiały Ceramiczne/Ceramic Materials/, 71(2), 127-144.

ANSYS, I. (2012). ANSYS Mechanical APDL Structural Analysis Guide.

Atoyebi, O. D., & Sadiq, O. M. (2018). Experimental data on flexural strength of reinforced concrete elements with waste glass particles as partial replacement for fine aggregate. Data in Brief, 18, 846-859.

Bangash, M. Y. H. (1989). Concrete and concrete structures: Numerical modelling and applications.

Bawab, J., Khatib, J., Jahami, A., Elkordi, A., & Ghorbel, E. (2021). Structural performance of reinforced concrete beams incorporating cathode-ray tube (CRT) glass waste. Buildings, 11(2), 67.

Baxter, S. Z., Meyer, C., & Jin, W. (1998). U.S. Patent No. 5,810,921. Washington, DC: U.S. Patent and Trademark Office.

Bažant, Z. P., Zi, G., & Meyer, C. (2000). Fracture mechanics of ASR in concretes with waste glass particles of different sizes. Journal of engineering mechanics, 126(3), 226-232.

Binici, H. (2007). Effect of crushed ceramic and basaltic pumice as fine aggregates on concrete mortars properties. Construction and Building Materials, 21(6), 1191-1197

Chen, M., Inoue, A., Zhang, W., & Sakurai, T. (2006). Extraordinary plasticity of ductile bulk metallic glasses. Physical review letters, 96(24), 245502.
Correia, J. R., De Brito, J., & Pereira, A. S. (2006). Effects on concrete durability of using recycled ceramic aggregates. Materials and Structures, 39(2), 169-177.
Correia, J. R., De Brito, J., & Pereira, A. S. (2006). Effects on concrete durability of using recycled ceramic aggregates. Materials and Structures, 39(2), 169-177.
Dahlén, L., & Lagerkvist, A. (2010). Pay as you throw: strengths and weaknesses of weight-based billing in household waste collection systems in Sweden. Waste Management, 30(1), 23–31.
Desayi, P., & Krishnan, S. (1964). Equation for the stress-strain curve of concrete. In Journal Proceedings, 61(3), 345–350.
Desayi, P., & Krishnan, S. (1964, March). Equation for the stress-strain curve of concrete. In Journal Proceedings (Vol. 61, No. 3, pp. 345-350).
García-González, J., Rodríguez-Robles, D., Juan-Valdés, A., Morán-del Pozo, J. M., & Guerra-Romero, M. I. (2015). Ceramic ware waste as coarse aggregate for structural concrete production. Environmental technology, 36(23), 3050-3059.
Gere, J. M., & Timoshenko, S. (1986). Theory of Elasticity 2nd ed. Grupo Editorial Iberoamérica.
Hama, S. M., Mahmoud, A. S., & Yassen, M. M. (2019, August). Flexural behavior of reinforced concrete beam incorporating waste glass powder. In Structures (Vol. 20, pp. 510-518). Elsevier.
Khaloo, A. R. (1995). Crushed tile coarse aggregate concrete. Cement, Concrete and Aggregates, 17(2), 119-125.
Kosmatka, S. H., & Wilson, M. L. (2011). Design and control of concrete mixtures. Portland cement Assoc.
Lee, H. (2015). Finite element simulations with ANSYS workbench 16. SDC publications.
Ling, T. C., Poon, C. S., & Wong, H. W. (2013). Management and recycling of waste glass in concrete products: Current situations in Hong Kong. Resources, Conservation and Recycling, 70, 25-31.
McCormac, J. C., & Brown, R. H. (2015). Design of reinforced concrete. John Wiley & Sons.
Meyer, C., and Baxter, S. (1998). ''Use of recycled glass and fly ash for precast concrete.'' Rep. NYSERDA 98-18 (4292-IABR-IA-96) to New York State Energy Research and Development Authority, Dept. of Civ. Engrg. and Engrg. Mech., Columbia University, New York.
Ohbuchi, Y., & Obikawa, T. (2003). Finite element modeling of chip formation in the domain of negative rake angle cutting. Journal of engineering materials and technology, 125(3), 324-332.
Ohbuchi, Y., & Obikawa, T. (2003). Finite element modelling of chip formation in the domain of negative rake angle cutting. Journal of Engineering Materials and Technology, 125(3), 324–332.
Senthamarai, R. M., & Manoharan, P. D. (2005). Concrete with ceramic waste aggregate. Cement and Concrete Composites, 27(9-10), 910-913.
Shayan, A. (2002). Utilisation of waste glass products in concrete. Municipal Engineering in Australia, 29(4).
Shi, C., & Zheng, K. (2007). A review on the use of waste glasses in the production of cement and concrete. Resources, conservation and recycling, 52(2), 234-247.
Standard, A. C. I. (1996). 211.1, Standard practice for selecting proportions for normal, heavyweight, and mass concrete. ACI Manual of Concrete Practice, Part, 1, 211-1.
Standard, A. S. T. M. (2006). Standard test method for water absorption, bulk density, apparent porosity and apparent specific gravity for fired white ware products. Annual Book ASTM Standard, 15, 112-3.
Standard, B. (1881). Part-102 (1983) Testing Concrete Method for Determination of Slump, London. British Standard Institution.
Subramani, T., & Ravi, G. (2015). Experimental Investigation of Coarse Aggregate with Steel Slag In Concrete. IOSR Journal of Engineering, 5(5), 64–73.
Topcu, I. B., & Canbaz, M. (2004). Properties of concrete containing waste glass. Cement and concrete research, 34(2), 267-274.
Wright, J. R., Cartwright, C., Fura, D., & Rajabipour, F. (2014). Fresh and hardened properties of concrete incorporating recycled glass as 100% sand replacement. Journal of Materials in Civil Engineering, 26(10), 04014073.
Zimbili, O., Salim, W., & Ndambuki, M. (2014). A review on the usage of ceramic wastes in concrete production. International Journal of Civil, Environmental, Structural, Construction and Architectural Engineering, 8(1), 91-95.

Int. J. of Sustainable Construction Engineering and Tech. Vol. 15 No. 2 (2024) p. 123-135

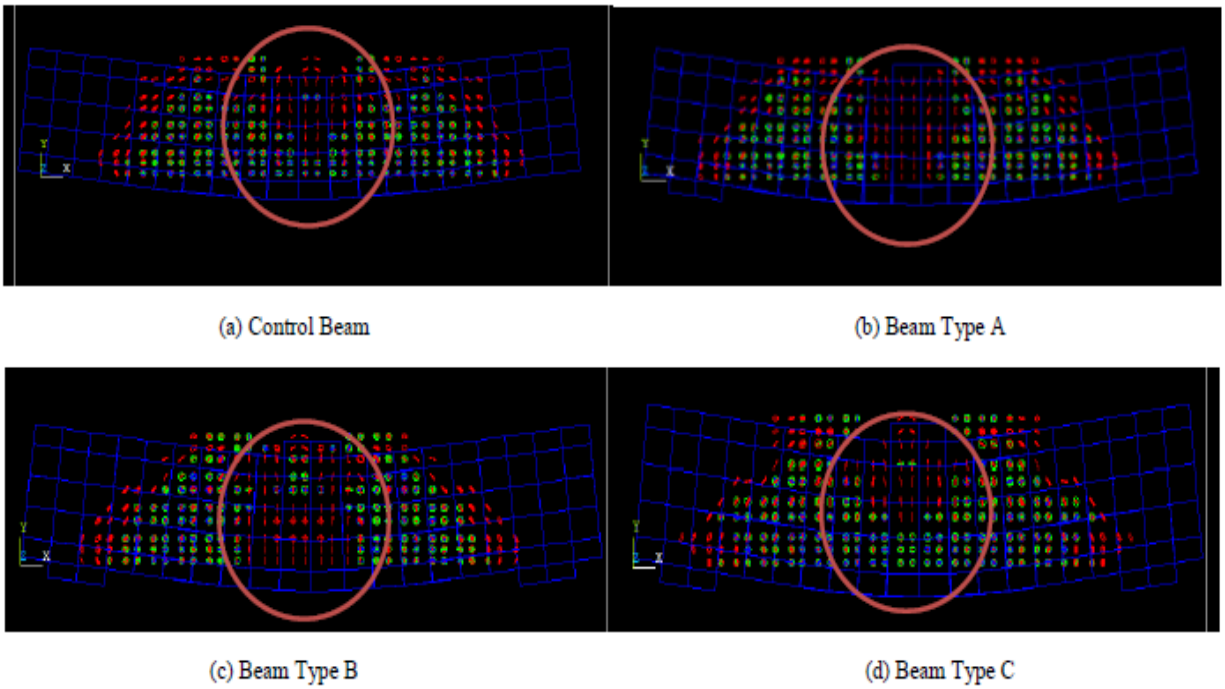

Fig. 14 *Crack patters of different types of beams, ANSYS*

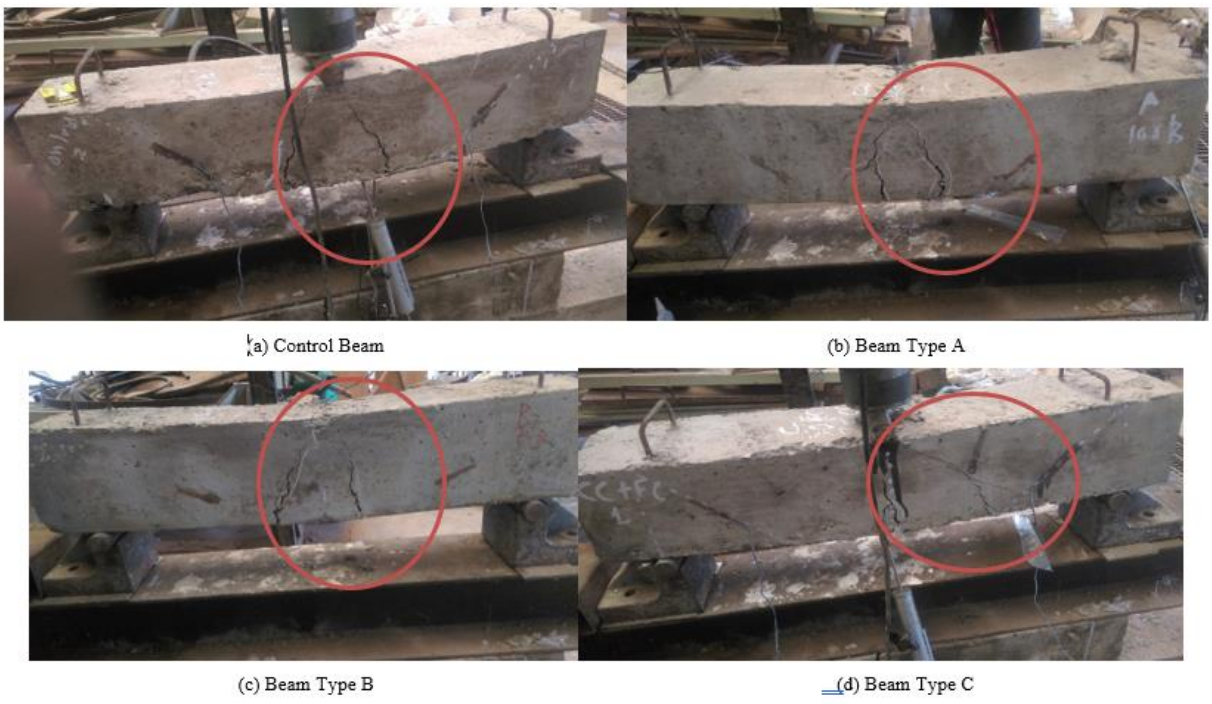

Fig. 15 *crack patters of different types of beams, experiment*